Design of the key components and optimization of the operating parameters for shielded boom sprayers

Wen Xiao[1,2†], Tao Xu[2†], Mengyu Wang[1,2], Haocheng Lu[3], Ming Dong[4], Xihan Li[5], Andreas Herbst[6], Xue Li[2,7*]

(1. *Faculty of Transportation Engineering, Huai'an University, Huaian 223003, China*;
2. *Institute of Agricultural Facilities and Equipment, Jiangsu Academy of Agricultural Sciences, Nanjing 210014, China*;
3. *College of Engineering, Nanjing Agricultural University, Nanjing 210031, China*;
4. *School of Automation, Nanjing University of Information Science and Technology, Nanjing 210044, China*;
5. *Jiangsu Pengtai Seed Industry Technology Co., Ltd, Nanjing 211225, China*;
6. *Julius Kuehn Institute - Institute for Application Techniques in Plant Protection, Braunschweig, Germany*;
7. *Key Laboratory of Modern Horticultural Equipment, Ministry of Agriculture and Rural Affairs, Nanjing 210014, China*)

Abstract: In order to address the problems of non-uniform droplet deposition and substantial drift loss during pesticide application on densely planted strawberry plants grown on wide ridges, a Shielded anti-drift spray boom was designed. A CFD model was constructed to simulate the airflow inside and outside the cover, and the effects of different cover widths on internal flow characteristics were analyzed to determine the optimal structural configuration. The simulation results indicated that the airflow inside the cover moves smoothly along the inner wall in a direction opposite to the sprayer's travel, forming an accelerated airflow zone at the rear lower edge of the cover. The downward-tilted airflow enhances droplet transport toward the canopy surface, while the vertical velocity component decreases with increasing cover width. A cover width of 50 cm produced the highest vertical velocity, which facilitated effective droplet deposition and reduced off-target drift. To further optimize the operating parameters and investigate the effects of spray angle, spray flow rate, and nozzle spacing on droplet deposition on strawberry leaves and stolons, this study conducted a Box–Behnken response surface experiment using artificial strawberry plants. The results showed that spray flow rate, spray angle, and nozzle spacing significantly affected leaf deposition, while flow rate had a notable influence on stolon deposition. The optimal operating parameters were a flow rate of 0.895 L/min, a spray angle of 30°, and a nozzle spacing of 35 cm, yielding deposition amounts of 4.16 μL/cm^2 on leaves and 0.12 μL/cm^2 on stolons, with coefficients of variation of 17.49% and 46.11%, respectively. Compared with the conventional boom sprayer in terms of anti-drift performance, the shielded sprayer had better anti-drift effect, which can effectively reduce the aerial drift of droplets by about 88.5% and the ground drift by about 68.6%.

Keywords: shielded spray, CFD simulation, droplet deposition, spray drift, anti-drift performance
DOI: 10.25165/j.ijabe.20261904.10378

Citation: Xiao W, Xu T, Wang M Y, Lu H C, Dong M, Li X H, et al. Design of the key components and optimization of the operating parameters for shielded boom sprayers. Int J Agric & Biol Eng, 2026; 19(4): 25–33.

1 Introduction

During the cultivation and plant protection management of strawberry plants, regular pesticide application is required to prevent diseases and pests that may lead to abnormal plant development. However, due to the unique growth morphology of strawberry plants, the dense canopy often obstructs spray droplet penetration during application. This obstruction reduces droplet penetration and results in insufficient deposition on both leaves and stolons, thereby lowering pest control efficacy. Shielded spraying has been recognized as an effective method to reduce pesticide drift and improve pesticide utilization. It mainly consists of pneumatic covering spray and mechanical covering spray. The former mainly uses the auxiliary airflow generated by some fan devices to change the original droplet movement trajectory and force the droplets to move towards the target crop. The latter mainly refers to changing the flow field distribution around the nozzle by adding a cover device around the nozzle, thereby reducing the drift of droplets and increasing the amount of droplet deposition[1]. This technology enhances droplet deposition and penetration, improves chemical control efficiency, and promotes spray uniformity[2].

Extensive research has been conducted domestically and internationally on cover-assisted spraying technologies to improve droplet deposition and reduce drift. Smith et al.[3] demonstrated that when auxiliary airflow reaches 7.1 m/s and natural wind speed is below 2 m/s, pneumatic shielded spraying significantly reduces droplet drift. Zhang et al.[4] optimized cover structures and showed

Received date: 2025-12-11 **Accepted date:** 2026-06-18
Biographies: Wen Xiao, MS candidate, research interest: vehicle performance optimization, Email: xw18796781263@163.com; **Tao Xu**, PhD candidate, research interest: plant protection machinery, Email: xutao@jaas.ac.cn; **Mengyu Wang**, MS candidate, research interest: vehicle performance optimization, Email: wmy18862001390@163.com; **Haocheng Lu**, MS candidate, research interest: precision spraying technology, Email: 2023812069@stu.njau.edu.cn; **Ming Dong**, MS candidate, research interest: intelligent manufacturing, Email: 17547625278@163.com; **Xihan Li**, Bachelor, research interest: agricultural engineering management, Email: pengtai-nursery@foxmail.com; **Andreas Herbst**, PhD, research interest: detection technology of plant protection machinery, Email: aherbst24@gmail.com.
†These authors contributed equally to this work.
***Corresponding author: Xue Li**, PhD, research interest: precision spraying technology. Institute of Agricultural Facilities and Equipment, Jiangsu Academy of Agricultural Sciences, Nanjing 210014, China. Tel: +86-15380827936, Email: lixue@jaas.ac.cn.

through repeated experiments that Shielded spraying outperforms conventional methods in reducing drift. Hu et al.[5] designed a conical airflow anti-drift device and verified through deposition tests that the design improves droplet retention. Fan et al.[6] developed a multi-airflow V-shaped anti-drift spray device for orchards and analyzed multiple factors affecting deposition, achieving substantial reductions in drift. Tsay et al.[7] used CFD to analyze droplet movement trajectories and airflow distributions under different cover geometries, while Sidahmed et al.[8] enhanced multi-foil symmetric covers to improve anti-drift performance. Wei[9] further designed a mechanical shield system and used FLUENT simulations to identify optimal operating conditions for Shielded spraying.

Most existing studies have focused on the effects of cover spray technology on droplet deposition and drift, using droplet deposition and simulation tests. By adjusting the cover geometry, airflow direction around the shield can be modified to reduce drift and improve deposition toward the target[10]. However, existing studies have mostly focused on general crops or orchard environments, and there is a lack of research on special windproof cover sprayers for the specific planting mode of "wide-ridge and dense-planting" field strawberry seedlings. In particular, the interaction between key operating parameters such as nozzle injection angle and spacing and the cover structure within the strawberry canopy has not been thoroughly explored, which leads to poor adaptability of existing equipment in strawberry fields and the need for improvement in deposition uniformity. Meanwhile, most spraying equipment for strawberry seedlings is ordinary boom sprayers without special anti-drift structures. Affected by natural wind during field operations, the aerial drift rate of fog droplets is as high as over 60%, and serious deposition occurs in non-target areas on the ground, which reduces the pesticide utilization rate. Therefore, this study aims to design a Shielded anti-drift boom sprayer suitable for densely planted strawberry plants on wide ridges. The airflow characteristics inside and outside the cover are analyzed using CFD, and droplet deposition and anti-drift performance tests are performed. The effects of spray angle, flow rate, and nozzle spacing on deposition performance are examined, and the optimal operating parameter combination for the Shielded sprayer is determined.

2 Test materials and methods

2.1 The sprayer

Strawberry seedlings in the field are planted using a wide ridge dense planting method[11], with ridge widths ranging from 1.3 to 1.5 m, a height of 0.35 m, and a spacing of 0.3 m between ridges. To improve droplet penetration during pesticide application, the sprayer must have good maneuverability[12]. Therefore, the sprayer's wheelbase should be adjustable between 1.5 m and 1.8 m to accommodate varying ridge widths. The operational diagram of the entire machine is shown in Figure 1.

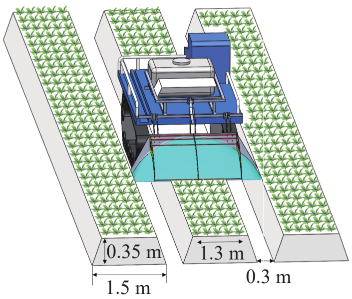

Figure 1 Driving diagram of the whole machine

The Shielded anti-drift spray boom sprayer consists of three primary subsystems: the track chassis, the power system, and the spray system. The track chassis includes crawler tracks and a hand-cranked mobile chassis that provides stable support and adjustable width. The power system comprises a gasoline engine and an electric drives assembly, ensuring reliable propulsion and operational stability. The spray system includes the cover, nozzles, medicine tank, plunger pump, pressure gauge, and associated piping components. The complete structure of the sprayer is illustrated in Figure 2. The integrated design ensures that the machine can operate efficiently within confined plantation rows while maintaining stable airflow and spray distribution under the cover.

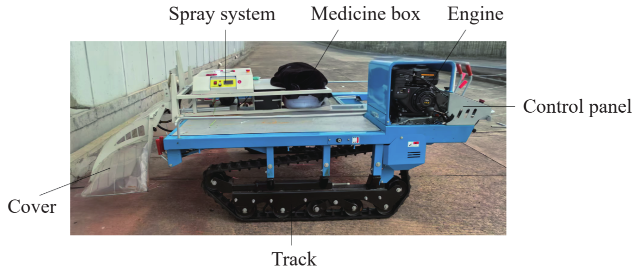

Figure 2 Cover type spray rod sprayer

The sprayer's track width can be adjusted via a lateral joystick to accommodate different strawberry ridge widths. A cover is mounted at the front of the sprayer, and three adjustable-angle nozzles (model: Lechler ST110-015) are installed beneath the cover. These nozzles are driven by a motor and supplied by a plunger pump (MSP T1000). By adjusting the pump's rotational speed, different spray flow rates can be achieved.

During operation, the cover guides the airflow to form a stable downward-oriented flow field. This guided airflow increases its velocity along the inner surface of the cover and applies downward pressure on droplets, enhancing their deposition on the leaves and stolons of strawberry plants. Simultaneously, the cover effectively reduces the lateral escape of droplets, thereby minimizing drift. The coordinated action of airflow guidance and nozzle orientation improves spray uniformity and deposition efficiency within the canopy.

2.2 Design of the shielding

To identify the optimal cover dimensions and investigate the airflow characteristics inside and outside the protective structure, a CFD simulation model of the airflow field was established using the fluid simulation software ANSYS FLUENT 2022[13]. The internal and external airflow fields of the cover were simulated and analyzed, and the airflow velocity was validated through bench testing.

2.2.1 Simulation of flow field

Given that the strawberry seedling ridges range from 1.3 and 1.5 m in width, the cover length was set to 1.5 m to fully span the ridge width. The ridge height is 0.35 m, and the track chassis has a ground clearance of approximately 1 m. During spraying, the lower edge of the cover must remain close to and level with the top of the strawberry canopy. Therefore, the vertical distance between the nozzles and the canopy was set to 30 cm, and the cover height was determined as 0.5 m. Based on these requirements, the external airflow domain was configured with dimensions of 2100 mm (length), 250 mm (width), and 650 mm (height), as shown in Figure 3.

The outer flow domain was meshed using unstructured tetrahedral elements generated through Fluent Meshing. The global grid size was set to 0.05 m, and five inflation layers were applied along the walls. A total of 131 174 cells were generated, with a skewness of 0.23 and an orthogonal quality of 0.99, meeting CFD grid quality requirements [14].

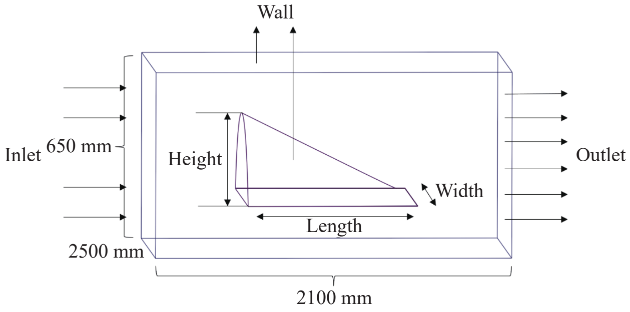

Figure 3 Area of the outflow field

During sprayer operation, the internal airflow travels downward along the inner front wall of the cover, while the external airflow moves backward along the outer surface. In the simulation, the inlet was set as a velocity inlet boundary with a flow speed of 0.5 m/s, and the outlet was defined as a pressure outlet. All solid surfaces, including the cover and machine components, were defined as no-slip walls. Air was selected as the working fluid. The solution employed a pressure-velocity coupled algorithm under steady-state conditions, using the standard k-ε turbulence model[15].

2.2.2 Grid independence verification

Grid independence verification is a crucial step to validate the reliability of calculation results in CFD simulations. To ensure that the simulation results are independent of the number of grid cells, three grids with different densities were designed for comparative analysis in this study. Grid generation was based on the same geometric model, and coarse, medium, and fine grids were generated by adjusting the grid cell size, respectively.

The average airflow velocity at the outlet section of the cover was selected as the monitoring index to compare the simulation results under the three types of grids. (Table 1)

Table 1 Comparison of three types of grids

Grid cell size/mm	Number of grid cells (10 000)	Average outlet wind speed/m·s^{-1}	Relative error/%
40	40.8	0.95	7.37
30	88.5	1.02	2.91
20	185	1.05	0.95

The results showed that due to the large cell size, the coarse grid (40 mm) failed to capture the detailed airflow characteristics, with a relatively low flow velocity of 0.95 m/s, and the relative error with the 30 mm grid reached 7.37% (≥5%). When the grid cell size was 30 mm, the flow velocity increased to 1.02 m/s, and the relative error dropped to 2.91% (≤5%), which met the requirements of grid independence. When the flow velocity of the fine grid converged further to 1.05 m/s, the relative error was only 0.95%, which verified the stability of the results. It also indicated that the grid cell size of 30 mm could well capture the flow field characteristics, and further grid refinement had a negligible impact on the results.

Considering the calculation accuracy and computational resources comprehensively, the medium grid with a cell size of 30 mm and a total number of 885 259 grid cells was selected for subsequent simulation analysis in this study.

2.3 Verification of simulation model

To validate the simulation results, a bench test platform was constructed (Figure 4), consisting of the protective cover, track system, motor, mobile trolley, control box, chemical tank, and associated components. Wind speed measurements were taken at three test points (Points 1, 3, and 5) located at the rear of the cover. A 405i hot-wire anemometer (Figure 5), with an accuracy of ± (0.3 m/s+5%), was used to record airflow velocities via Bluetooth. For each point, the average wind speed recorded during a stable 3-5 s interval was taken as the measured value, and each location was tested six times.

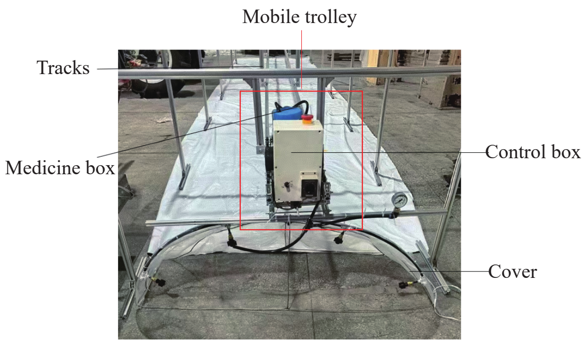

Figure 4 Schematic diagram of the bench

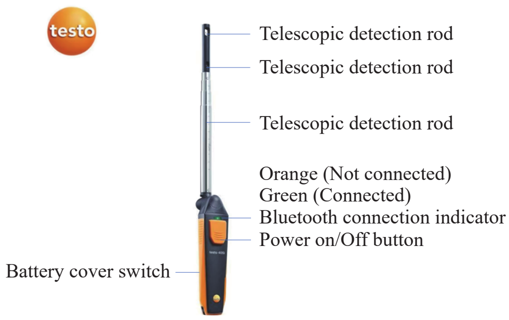

Figure 5 Testo 405i anemometer

2.4 Optimization of sprayer operational parameters

Based on the CFD simulation and bench test results, the cover dimensions were finalized as 1.5 m in length, 0.5 m in width, and 0.5 m in height. To further evaluate the effects of spray angle, flow rate, and nozzle spacing on droplet deposition on strawberry leaves and stolons, a Box-Behnken response surface experimental design was applied. The interactions among different parameters were examined to determine the optimal operating conditions for the Shielded anti-drift sprayer.

2.4.1 Experimental design

To systematically explore the influence law of the interaction among various factors on the droplet deposition distribution of strawberry seedlings, a three-factor, three-level Box-Behnken response surface experiment was designed in combination with the planting characteristics and canopy structural features of strawberry seedlings under the wide-ridge and dense-planting pattern.

Spray inclination angle, nozzle flow rate, and nozzle spacing are the core operating parameters affecting the droplet deposition distribution and drift characteristics of boom sprayers. Numerous studies have confirmed that these three parameters exert a significant regulatory effect on the droplet deposition amount, deposition uniformity, and penetration on target crops, and they are also the key research objects for the optimization of plant protection spray parameters. Among them, the spray inclination angle directly determines the droplet ejection trajectory, and adjusting the angle can alter the coverage range and penetration of droplets on the crop canopy. Especially for the growth characteristics of strawberry seedlings, such as severe canopy shielding and stolons distributed in the lower layer, a reasonable inclination angle setting can effectively improve the droplet deposition effect on the lower target. Therefore, the spray angles selected in this study were based on the structural characteristics of the strawberry canopy and existing research on the effect of nozzle inclination angle on deposition, with three levels of 0°, 15°, and 30° adopted[16]. The nozzle flow rate not only determines the pesticide application rate per unit time, but also its variation can further affect the droplet drift characteristics and canopy adhesion capacity. In this study, the flow rates were set at 0.43 L/min, 0.66 L/min, and 0.90 L/min mainly based on the adjustable range of the equipment, which can achieve the particle size variation from fine to coarse droplets. Nozzle spacing determines the lateral distribution uniformity of droplets on the ridge surface, and its setting must match the crop ridge width to ensure full coverage of droplets without missing or excessive overlapping, serving as a fundamental parameter for improving the quality of field spray operations. In this study, the nozzle spacing was set according to the strawberry ridge width and common boom configurations[17], with three levels of 30 cm, 35 cm, and 40 cm selected to cover the entire width of the strawberry canopy and match the strawberry planting pattern with a ridge width of 1.3 m to 1.5 m.

Spray angle (*A*), flow rate (*B*), and nozzle spacing (*C*) served as the independent variables. Tables 2 and 3 list the coded factor levels and the experimental matrix.

Table 2 Coding of each level

Level	Spray angle/(°)	Nozzle flow rate/L·min^{-1}	Spacing/cm
–1	0	0.43	30
0	15	0.66	35
1	30	0.90	40

Table 3 Experimental design scheme

Code	Factor		
	A	*B*	*C*
1	–1	–1	0
2	1	–1	0
3	–1	1	0
4	1	1	0
5	–1	0	–1
6	1	0	–1
7	–1	0	1
8	1	0	1
9	0	–1	–1
10	0	1	–1
11	0	–1	1
12	0	1	1
13	0	0	0
14	0	0	0
15	0	0	0
16	0	0	0
17	0	0	0

To minimize the influence of environmental factors such as ambient wind, humidity, and temperature[18,19], indoor spray tests were conducted in a 1.5 m×1.2 m testing area using artificial strawberry plants. Before the experiment, strawberry plants were arranged in three rows with 60 cm spacing. Five sampling points were uniformly distributed along each row. Filter paper (9 cm in diameter) was randomly placed on the leaf surface, while 5 cm-long PTFE wires were placed beneath the leaves to represent stolons. In each trial, 30 samples were collected. Figures 6 and 7 illustrate the experimental setup. A 2‰ aqueous carmine dye solution served as the spray tracer[20].

Figure 6 Schematic diagram of sample arrangement

Figure 7 Distribution map of strawberry plants

To evaluate the anti-drift performance of the cover under the optimal parameters, a comparative test on the airborne drift and ground drift of the cover spray and the ordinary spray rod spray was carried out: A total of 15 points (3×5) of Teflon wire with a diameter of 2 mm and a height of 25 cm, 45 cm, 65 cm, 85 cm, and 105 cm from the ground are arranged 1 meter away from the cover in the downstream wind direction[21], as shown in Figure 8. The filter paper is arranged at intervals of 1 m in front, back, left, and right on the ground. The test parameters adopted the optimal spray parameters: the spacing was 35 cm, the flow rate was 0.895 L/min, and the spray angle was 30°. The test was conducted on a sunny and windy day with a wind speed of 19 km/h and a temperature ranging from 26°C to 34°C. After each group of experiments is completed, the filter paper and Teflon wire are collected and stored in plastic sealed bags.

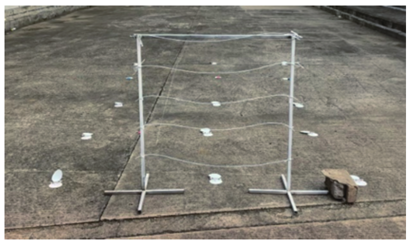

Figure 8 Distribution of drift sample points

2.4.2 Data processing

Deionized water was used to elute the target. The concentration of carmine-red eluent was determined at a wavelength of 512 nm using a 722 s spectrophotometer. Droplet deposition and the coefficient of variation[22,23] were calculated according to Equations (1) and (2). The experimental data were processed and analyzed using Design-Expert13 software.

$$d = \frac{V_W \cdot F_{Ls}}{N \cdot F_{La} \cdot S} \times 10^3 \tag{1}$$

where, V_W represents the volume of the liquid to be tested, mL; F_{LS} represents the absorbance value; N represents the dilution factor; F_{La} represents the absorbance value of the mother liquor; and S represents the area of the culture dish, cm^2.

$$\text{CV} = (s/\bar{q}) \times 100\% \tag{2}$$

where, s represents the standard deviation of the sample; and $\bar{q}$ represents the mean of the sample.

$$P = n/N \times 100\% \tag{3}$$

where, P is the deposition rate; n is the pesticide dose deposited on the surface of the target crop; N is the total application rate of the pesticide.

3 Analysis of test results

3.1 Simulation results and analysis

Three cover widths (0.5 m, 0.8 m, and 1.0 m) were selected for internal and external airflow field simulations. The particle trace diagrams for internal and external flow fields are shown in Figures 9 and 10.

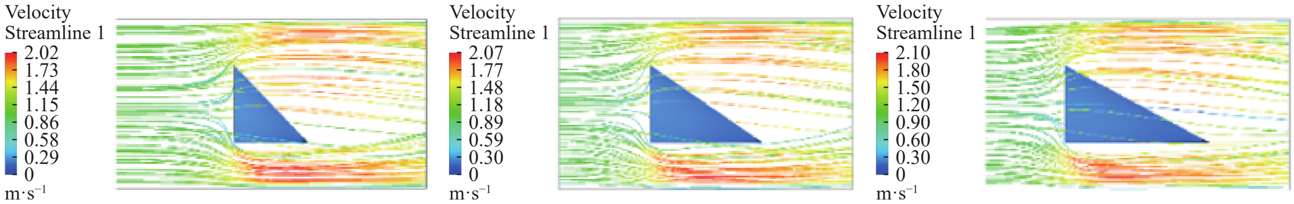

a. 0.5 m b. 0.8 m c. 1.0 m

Figure 9 Traces of the outflow field

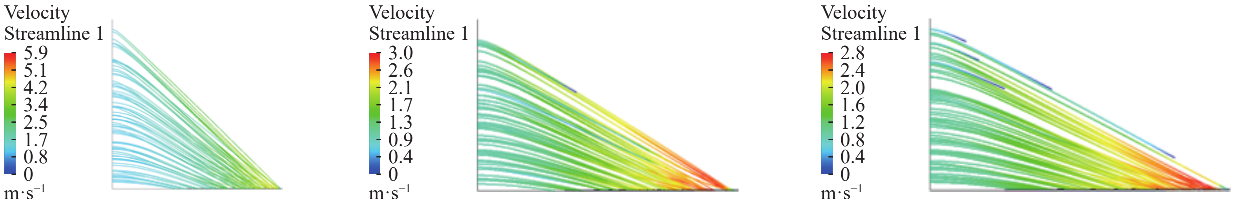

a. 0.5 m b. 0.8 m c. 1.0 m

Figure 10 Trace of the internal flow field

According to the simulation results, it can be seen that the airflow inside the cover follows the inner contour smoothly and moves opposite to the forward motion of the sprayer. An accelerated airflow zone generates at the rear lower portion of the cover, directing droplets toward the canopy. The airflow vector tilts downward along the tangent of the curved cover wall, enhancing downward droplet transport. To compare airflow characteristics among the three cover widths, five test points located 0.05 m behind the cover were selected, with horizontal spacing of 0.3 m between points, as illustrated in Figure 11.

As shown in Figure 12, the vertical velocity at all points is substantially higher than the horizontal component, indicating rapid droplet settling[24]. In addition, the vertical velocity magnitude decreases as cover width increases, demonstrating that reducing the cover width enhances internal airflow velocity and thus accelerates droplet deposition. The 0.5 m cover exhibited the smallest horizontal airflow velocity, which is beneficial for minimizing lateral drift.

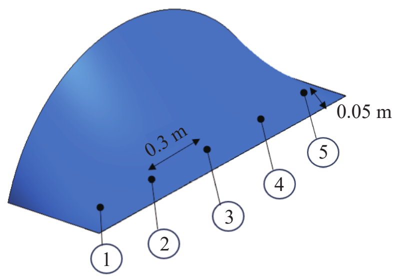

Note: 1 to 5 in the figure represent the positions of the measured points.

Figure 11 Schematic diagram of the five point positions

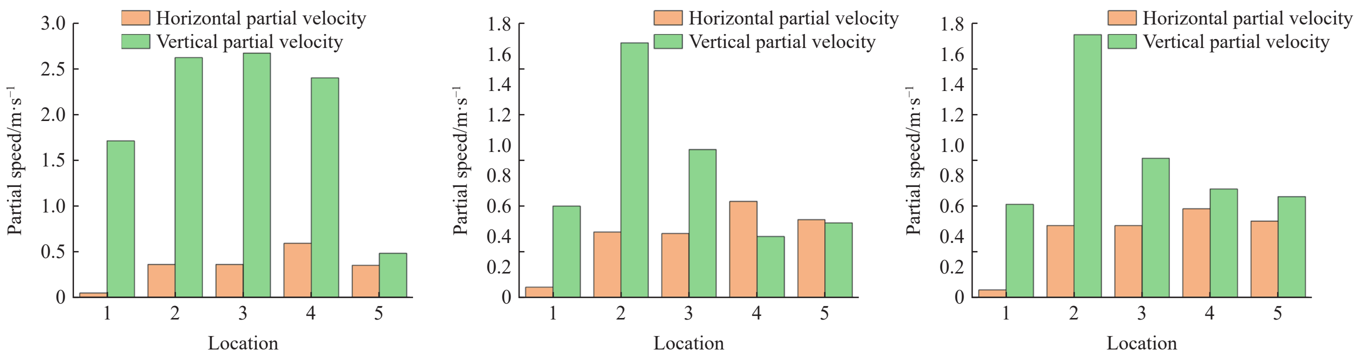

a. 0.5 m b. 0.8 m c. 1.0 m

Figure 12 Bar graph of fractional velocity comparison

3.2 Analysis of verification results

The data measured in the verification test were compared with those in the above simulation test. The measured data are listed in Table 4.

Table 4 Simulation values and measured values

Site	Simulation/m·s⁻¹	Measured/m·s⁻¹						Average/m·s⁻¹
1	1.17	1.09	1.11	1.03	1.04	1.12	1.09	1.08
3	1.43	1.36	1.45	1.34	1.50	1.48	1.39	1.42
5	0.55	0.50	0.47	0.45	0.49	0.36	0.43	0.45

A linear regression analysis was performed between the simulated and measured values. As shown in Figure 13, the coefficient of determination (R^2) reached 0.947 16, indicating a strong correlation between simulation and experiment. The deviations between simulated and measured values were small and statistically insignificant, confirming the validity and reliability of the CFD model[25].

3.3 Analysis of optimization results

3.3.1 Significance analysis

Table 5 summarizes the experimental results, while Table 6 presents the corresponding significance analysis.

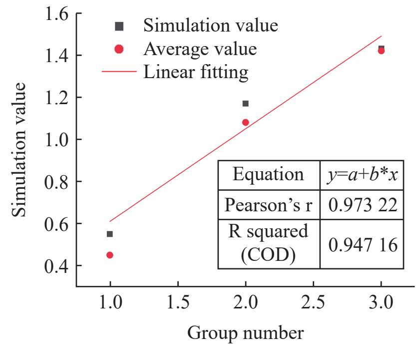

Figure 13 Linear fitting diagram

Table 5 Test results of droplet deposition volume

Code	Factor A	Factor B	Factor C	Leaf deposition/ (μL·cm⁻²)	Stolon deposition/ (μL·cm⁻²)	Coefficient of variation of leaves/%	Coefficient of variation of stolons/%	Leaf deposition rate/%	Stolon deposition rate/%
1	–1	–1	0	3.39	0.05	18.75	27.70	38.26	27.78
2	1	–1	0	3.36	0.04	42.07	38.30	37.92	22.22
3	–1	1	0	5.01	0.12	53.59	51.20	56.74	66.67
4	1	1	0	4.76	0.12	17.49	46.11	53.9	66.67
5	–1	0	–1	2.75	0.06	20.45	30.21	39.97	33.33
6	1	0	–1	2.67	0.05	7.19	26.38	38.85	27.78
7	–1	0	1	2.74	0.05	54.15	57.16	39.83	27.78
8	1	0	1	2.59	0.04	62.03	68.44	37.72	22.22
9	0	–1	–1	1.92	0.06	27.98	70.73	21.76	33.33
10	0	1	–1	3.58	0.10	24.14	25.03	40.64	55.56
11	0	–1	1	1.88	0.04	77.1	70.83	21.3	22.22
12	0	1	1	3.49	0.11	24.32	50.38	39.64	61.11
13	0	0	0	2.30	0.06	28.09	74.92	33.31	33.33
14	0	0	0	2.35	0.08	8.13	36.80	34.04	44.44
15	0	0	0	2.34	0.05	22.64	39.80	33.89	27.78
16	0	0	0	2.36	0.06	46.05	50.91	34.19	33.33
17	0	0	0	2.33	0.07	28.31	49.10	33.75	38.89

Note: Leaf deposition represents the data measured by filter paper; stolon deposition represents the data measured by polytetrafluoroethylene (PTFE) threads.

Table 6 Significance analysis table of droplet deposition

Source	Sum of squares		Degrees of freedom		Mean square		*F* value		*p*-value	
	Deposition amount	Stolon	Deposition amount	Stolon	Deposition amount	Stolon	Deposition amount	Stolon	Deposition amount	Stolon
Model	12.87	0.0114	9	9	1.43	0.0013	6217.32	12.05	< 0.0001	0.0017
A	0.0235	0.0001	1	1	0.0235	0.0001	102.00	0.9121	< 0.0001	0.3714
B	4.90	0.0085	1	1	4.90	0.0085	21 294.69	80.51	< 0.0001	<0.0001
C	0.0038	0.0001	1	1	0.0038	0.0001	16.31	0.9121	0.0049	0.3714
AB	0.0121	0.0000	1	1	0.0121	0.0000	52.60	0.2382	0.0002	0.6404
AC	0.0013	1.352E-06	1	1	0.0013	1.352E-06	5.83	0.0129	0.0464	0.9128
BC	0.0016	0.0002	1	1	0.0016	0.0002	6.96	2.14	0.0336	0.1866
A^2	3.29	0.0001	1	1	3.29	0.0001	14 282.61	0.7108	< 0.0001	0.4271
B^2	3.46	0.0022	1	1	3.46	0.0022	15 046.49	20.69	< 0.0001	0.0026
C^2	1.21	0.0004	1	1	1.21	0.0004	5271.60	3.40	< 0.0001	0.1076
Residuals	0.0016	0.0007	7	7	0.0002	0.0001				
Missing items	0.0006	0.0002	3	3	0.0002	0.0001	0.8136	0.5506	0.5494	0.6743
Error	0.0010	0.0005	4	4	0.0003	0.0001				
Total	12.87	0.0121	16	16						

Note: 1. *A* represents spray angle; *B* represents flow rate; *C* represents spacing; 2. $p < 0.0001$ indicates that the factor or model is highly significant.

Regression analysis of the 17 experimental groups yielded the following quadratic models for leaf deposition (Y_1) and stolon deposition (Y_2):

$$Y_1 = 2.34 - 0.0542A + 0.7825B - 0.0217C - 0.0550AB - 0.0183AC - 0.0200BC + 0.8833A^2 + 0.9067B^2 - 0.5367C^2 \quad (4)$$

$$Y_2 = 0.064 + 0.0325B + 0.0227B^2 \quad (5)$$

Based on the obtained regression model, significance analysis was conducted to determine the significant influence of each factor on the deposition amount, stolon deposition, and coefficient of variation.

According to Table 5, the p-value of the deposition model is less than 0.0001, and the lack-of-fit p-value is 0.5494 (p>0.05), indicating that the predictive model is highly significant and statistically meaningful. For droplet deposition, the p-values corresponding to factors A, B, A^2, B^2, and C^2 are all less than 0.0001, showing an extremely significant impact on droplet deposition. Factors C, AB, AC, and BC have p-values less than 0.005, indicating a significant effect on droplet deposition. For stolon deposition, the model p-value is 0.0017 (less than 0.005), which is significant. Among these, factor B has a p-value less than 0.0001, showing a significant impact on stolon deposition, while other factors have no significant effect.

Significance analysis indicated that spray angle (A), flow rate (B), and nozzle spacing (C) all had highly significant effects on leaf deposition. Flow rate showed a significant effect on stolon deposition, whereas spray angle and spacing had lesser influence.

3.3.2 Response surface model analysis

The response surface plots corresponding to the interaction effects of the three parameters are shown in Figure 14.

As shown in Figure 14a, for the interaction between spray inclination angle (A) and spray flow rate (B): at the same inclination angle, the droplet deposition on leaves exhibited a trend of first decreasing and then increasing with the rise in flow rate. When the flow rate increased from 0.43 L/min to 0.90 L/min, the leaf deposition rate rose from 21.30%-27.78% to 39.64%-66.67%, and the stolon deposition rate increased from 22.22%-33.33% to 55.56%-66.67% simultaneously. This indicated that the optimization of flow rate not only increased the pesticide application volume, but also improved the pesticide utilization rate by enhancing the droplet penetration and targeting performance. At the same flow rate, the droplet deposition also showed a trend of first decreasing and then increasing with the increase in inclination angle. In summary, the droplet deposition reached the maximum value of 4.805 mL/cm² when the flow rate was 0.90 L/min and the inclination angle was 30°. The main reason was that the number of droplets was insufficient at low flow rates, so the deposition could only be improved slightly even if the inclination angle was adjusted; at high flow rates, the 30° inclination angle enabled the droplets to accurately cover the crop canopy and avoid drift loss.

For the interaction between spray angle (A) and nozzle spacing (C) (Figure 14b): at the same spray angle, the deposition amount first increased and then decreased with the increase in nozzle spacing; at the same nozzle spacing, the deposition amount first decreased and then increased with the increase in spray angle. The deposition amount peaked at a nozzle spacing of 35 cm and a spray angle of 30°. This is because the 35 cm nozzle spacing matches the row width of wide strawberry ridges, resulting in a moderate degree of droplet overlap, and the comprehensive coverage of the strawberry canopy can be achieved in combination with a 30° spray angle.

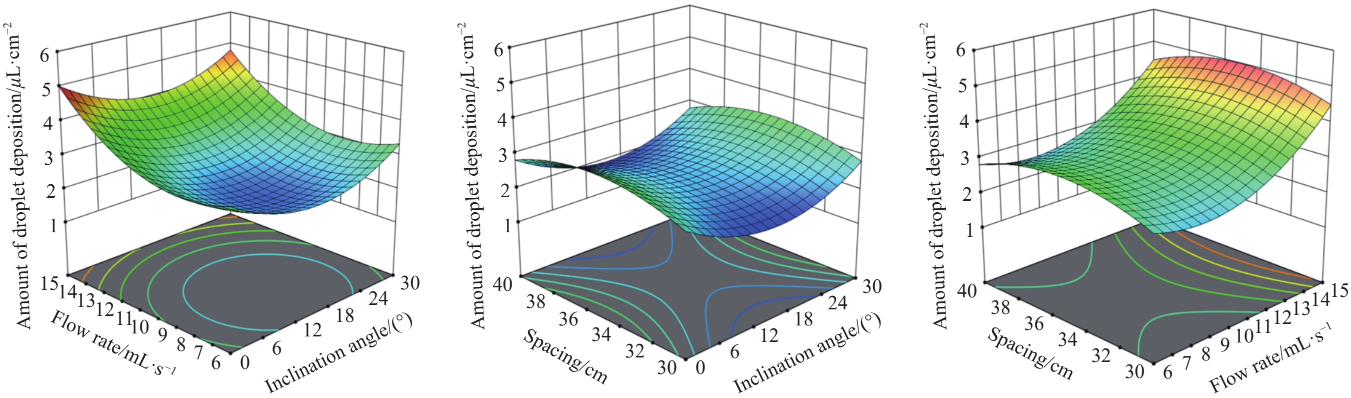

Note: A factor value of 0 indicates that the factor remains unchanged.

Figure 14 Response surface model

As for the interaction between flow rate (B) and nozzle spacing (C) (Figure 14c): at the same flow rate, the deposition amount first increased and then decreased with the increase in nozzle spacing; at the same nozzle spacing, the deposition amount first decreased and then increased with the increase in flow rate. The deposition amount reached the maximum at a nozzle spacing of 35 cm and a flow rate of 0.90 L/min, where the droplets were sufficient and uniformly distributed without aggregation in overlapping areas or missed spraying.

Through Box-Behnken response surface experiments and regression fitting analysis, it was determined that droplet deposition is influenced by spray flow rate, spray inclination angle, and spray spacing. Under the combination of minimum flow rate and minimum inclination angle, the coefficient of variation was as high as 77.10%; while under the combination of high flow rate and high inclination angle, the coefficient of variation decreased to 17.49%. This indicates that appropriately increasing the flow rate and inclination angle can significantly improve droplet deposition uniformity. However, excessively high parameter combinations may lead to localized over-deposition, which in turn reduces spray uniformity. Based on Design-Expert 13.0 software, the optimal parameter combination for the covered anti-drift boom sprayer was determined as follows: spacing of 35 cm, flow rate of 14.92 mL/s, and inclination angle of 30°, with a coefficient of variation of 17.49%, which meets the sprayer operation quality standard (coefficient of variation of droplets ≤ 50%) [26].

3.3.3 Analysis of drift loss results

Based on the comparative test results of anti-drift performance, Figure 15 indicates that the Shielded spray system drastically reduces both airborne drift and ground drift compared to the conventional spray system. The airborne droplet drift[27] for the Shielded spray system was approximately 0.08 μL/cm², and the ground drift was about 0.065 μL/cm². In contrast, conventional spray rods had significantly higher drift values. The Shielded system effectively reduced airborne droplet drift by 88.5% and ground drift by 68.6%, demonstrating its superior anti-drift performance.

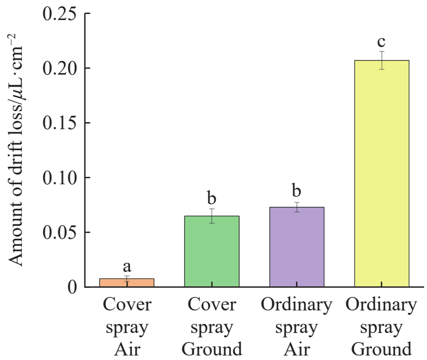

Note: Different lowercase letters indicate significant differences between groups (p<0.05); error bars represent standard deviation, n=3.

Figure 15 Comparison of drift

4 Discussion

In recent years, many scholars at home and abroad have carried out extensive research on wind-shield sprayers. Although various cover structures have achieved the goal of reducing droplet drift, there are still some differences in their flow field regulation capabilities and target adaptability due to the influence of design objects and structural forms. The covered boom sprayer designed in this study forms unique advantages in terms of cover structure, directional airflow guidance, and adaptability to wide-ridge and dense-planted crops.

(1) From the perspective of the cover flow field regulation mechanism, the existing wind-shield sprayers mostly adopt the modes of air-assisted pressurization or large-size wide-width flow guidance. Although these modes can reduce droplet drift, they have the problems of high-power consumption of the whole machine and mismatched structural size with dwarf and dense-planted crops. Based on the growth characteristics of strawberry seedlings in wide-ridge and dense-planted fields, this study designed a semi-closed cover without air assistance. The directional flow guidance of the cover wall realizes the downward pressure and acceleration of airflow, which not only avoids additional power consumption, but also adapts to the operation space between strawberry ridges through the 0.5 m narrow-width design. Meanwhile, the obliquely downward airflow direction at the rear end of the cover can effectively transport droplets to the stolons in the lower layer of strawberry plants, solving the problem of insufficient deposition on the lower target of dwarf crops by the existing wind-shield sprayers.

(2) At present, the mainstream pesticide application technologies for strawberry seedlings in wide-ridge and dense-planted fields are mainly the ordinary boom spray technology and the unmanned aerial vehicle (UAV) low-altitude spray technology. Due to the lack of anti-drift structure, the ordinary boom spray technology has a droplet aerial drift rate of more than 60% under the influence of natural wind. In addition, droplets are easily blocked by the strawberry canopy, resulting in extremely low deposition on stolons, which is difficult to meet the needs of pest and disease control. Although the UAV low-altitude spray technology has high operation efficiency, it has the disadvantages of small droplet size, great influence by high-altitude wind, and poor droplet penetration, making it impossible for droplets to effectively reach the stolons in the lower layer of strawberry plants.

5 Conclusions

This study addressed the challenges of uneven droplet deposition and substantial spray drift during pesticide application in densely planted strawberry fields with wide ridges. A Shielded anti-drift boom sprayer was designed, and its structural parameters and operating conditions were optimized through CFD simulations, bench verification, and response surface experiments. The main conclusions are as follows:

(1) CFD analysis demonstrated that a 0.5 m cover width generated a strong downward airflow with significantly greater vertical velocity than horizontal velocity, promoting rapid droplet deposition while minimizing lateral drift. The airflow pattern under this configuration effectively enhanced on-target deposition.

(2) Box–Behnken response surface experiments showed that spray angle, flow rate, and nozzle spacing all had significant effects on leaf deposition. Flow rate exhibited a notable influence on stolon deposition. The optimal combination of parameters was determined to be a nozzle spacing of 35 cm, a flow rate of 14.92 mL/s, and a spray angle of 30°, yielding uniform droplet deposition with a leaf deposition coefficient of variation of 17.49%.

(3) Comparative drift tests demonstrated that the Shielded sprayer substantially reduced both airborne and ground drift relative to a conventional boom sprayer. Airborne drift was reduced by 88.5%, and ground drift was reduced by 73.2%, confirming the strong anti-drift capability of the cover structure.

(4) The covered boom spray technology designed in this study reduces the aerial drift rate to less than 11.5% and the ground non-target deposition rate to less than 26.8% through the anti-drift and flow guidance effect of the cover. Meanwhile, through the optimization of operation parameters, the coefficient of variation of droplet deposition on leaves is reduced to 17.49%, which is much lower than that of the ordinary boom spray technology. In addition, the adjustable wheel track design of the crawler chassis is adapted to the 1.3-1.5 m strawberry ridge width, solving the problem of poor inter-ridge passability of the existing pesticide application equipment, and realizing precise, efficient, and low-drift pesticide application in wide-ridge and dense-planted strawberry fields.

(5) Based on the results of this study, in-depth research can be carried out from three aspects in the future. First, optimize the bionic structural design of the cover, and design a variable-curvature arc cover combined with the canopy morphology of strawberry seedlings to further improve the flow field guidance efficiency and the uniformity of droplet deposition. Second, carry out field experiments on multi-factor coupling, explore the coupling effect of environmental factors such as natural wind speed, temperature, and humidity with operation parameters, and establish a dynamic regulation model of field operation parameters. Third, develop an intelligent pesticide application system, integrate the functions of automatic nozzle flow regulation and adaptive cover height, and realize intelligent and precise pesticide application in wide-ridge and dense-planted strawberry fields.

Acknowledgements

This work was supported by Jiangsu Provincial Science and Technology Project on Modern Agriculture (BE2023304) and the National Key Research and Development Program of China (2024YFD200010025).

[References]

[1] Li L L, Chen L P, Zhang R R, Tang Q, Yi T C, Liu B Q, et al. Spray drift characteristics of pulse-width modulation sprays in windtunnel. Int J Agric & Biol Eng, 2022; 15(4): 7–15.

[2] Li H Z, Zhu H, Jiang Z H, Lan Y B. Performance characterization on downwash flow and spray drift of multirotor unmanned agricultural aircraft system based on CFD. Int J Agric & Biol Eng, 2022; 15(3): 1–8.

[3] Smith D B, Harris F D, Butler B J. Shielded sprayer boom to reduce drift. Transactions of the ASAE, 1982; 25(5): 5–16.

[4] Zhang J, Yang X L, He X K, Song J L. Experiment on reducing droplet drift by improving double arc cover. Transactions of the CSAM, 2009; 40(7): 67–71. (in Chinese)

[5] Hu J, Liu C X, Chu X, Li Y F, Sun S Y, Zhang W. Research on droplet deposition characteristics of conical wind field anti-drift device. Transactions of the CSAM, 2020; 51(12): 142–149, 174. (in Chinese)

[6] Fan G J, Niu C C, Zhang Z M, Wang D W, Mao W H, Jiang H H. Design and experiment of multi-airflow cooperative v-shaped anti-drift spray device for orchards. Transactions of the CSAM, 2022; 53(3): 138–147. (in Chinese)

[7] Tsay J, Ozkan H E, Fox R D. CFD simulation of mechanical spray shields. Transactions of the ASAE, 2002; 45(5): 1271.

[8] Sidahmed M M, Awadalla H H, Haidar M A. Symmetrical multi-foil shields for reducing spray drift. Biosystems Engineering, 2004; 88(3): 305–312.

[9] Wei X P. CFD simulation and experiment of shields spray system. Xianyang: Northwest A&F University, 2021. DOI: 10.27409/d.cnki.gxbnu.2021.001866. (in Chinese)

[10] Tao L. Theoretical and experimental research on reducing droplet drift of medicinal liquid with arc-shaped covers. China Agricultural University, 2004. (in Chinese)

[11] Jia M S, Zhang L J, Dun G Q, Gao S, Huang X W, Wang S Y. Design and trajectory simulation reliability analysis of self-propelled strawberry sprayer. Chinese Journal of Agricultural Mechanization, 2023; 44(7): 85–90, 117. (in Chinese)

[12] Qiu W, Zhang K L, Lu Q, Huang X R, Deng Y J, Zhou L F, et al. Design and test of goose-neck long-range air-assisted sprayer for nursery. Transactions of the CSAE, 2024; 40(20): 46–53. (in Chinese)

[13] Li S Z. Development of traditional apple orchard air-driven sprayer based on CFD flow field simulation. Northwest A&F University, 2018. DOI: 10.27409/d.cnki.gxbnu.2018.000068. (in Chinese)

[14] Wu S X, Zhang K P, Wang J X. Design and simulation analysis of self-propelled mist sprayer for orchards. Journal of Jilin University (Engineering and Technology Edition), 2025; 55(11): 3762–3773. (in Chinese)

[15] Chu X. Experimental study on the spray performance of conical airflow auxiliary device. Heilongjiang Bayi Agricultural University, 2020. DOI: 10.27122/d.cnki.ghlnu.2020.000099. (in Chinese)

[16] Bian Z H, Lan Y B, Wang M, Shan C F, Gu H Z, Han J G. Effect of nozzle angle of plant protection unmanned aerial vehicle on droplet deposition distribution. Open Academic Journals Index, 2024; 72(1): 214–223.

[17] Zhu F Y, Wu G, Ji Y H, Xie L, Ban Z J, Liang H. Numerical simulation and experimental study of spray deposition distribution characteristics of vertical spray in greenhouses. Journal of Chinese Agricultural Mechanization, 2025; 46(11): 171–177, 187. (in Chinese)

[18] Qi L J, Hu J R, Shi Y, Fu Z T. Correlation analysis between spray parameters and drift. Transactions of the CSAE, 2004; 20(5): 122–125. (in Chinese)

[19] Ministry of Industry and Information Technology of the People's Republic of China. Equipment for crop protection - General test methods. JB/T 9782-2014, 2014.

[20] Wang J, Dong X, Yan H R, Wang J J, Zhang T, Zeng Y H. Experiment on pesticide application in corn field by wind curtain boom sprayer. Transactions of the CSAM, 2015; 46(7): 79–84. (in Chinese)

[21] Standardization Administration of the People's Republic of China. Equipment for crop protection - Methods for field measurement of spray drift. GB/T 24681-2009/ISO 22866: 2005, 2009.

[22] Zhang L, Liu J R, Li Z Y, Teng F, Zhao J W. Research on the operation quality of different spraying methods for greenhouse strawberries. Chinese Journal of Agricultural Mechanization, 2023; 44(7): 63–68. (in Chinese)

[23] Li L L, He X K, Song J L, Liu Y, Wang Z C, Li J Y, et al. Comparative test on the performance of conformational variable spray and conventional air-assisted spray in orchards. Transactions of the CSAE, 2017; 33(16): 56–63. (in Chinese)

[24] Yang X L. Research on theory and trial of double-foil shield in reducing spray drift. China Agricultural University, 2005. (in Chinese)

[25] Zhu X Y, Zhao Y, Li X Y, Qian Z, Liu J P. Experimental study on spray deposition characteristics of self-propelled boom sprayer. Journal of Drainage and Irrigation Machinery Engineering, 2025; 43(1): 94–100. (in Chinese)

[26] Ministry of Agriculture of the People's Republic of China. Operating quality for sprayers. NY/T 650-2002, 2002. (in Chinese)

[27] Song Y Y. Analysis of air curtain system flow field and droplet drift characteristics of high clearance sprayer based on CFD. Int J Agric & Biol Eng, 2024; 17(6): 38–45.